

## GENUINE IRREGULAR GALAXIES AS A RELIC OF BUILDING BLOCKS OF GALAXIES

K. TERA<sup>1</sup>, Y. TANIGUCHI<sup>2</sup>, M. KAJISAWA<sup>1,2</sup>, Y. SHIOYA<sup>2</sup>, M. A. R. KOBAYASHI<sup>2</sup>, K. MATSUOKA<sup>4</sup>, H. IKEDA<sup>1,5,6</sup>, K. L. MURATA<sup>3</sup>, A. ICHIKAWA<sup>1</sup>, M. SHIMIZU<sup>1</sup>, M. NIIDA<sup>1</sup>, AND E. HAMAGUCHI<sup>1</sup>

*Draft version January 17, 2018*

### ABSTRACT

In order to understand nature of building blocks of galaxies in the early universe, we investigate “genuine irregular galaxies (GIGs)” in the nearby universe. Here, GIGs are defined as isolated galaxies without regular structures (spheroid, bulge, disk, bar, spiral arm, and nucleus). Using the results of two excellent studies on galaxy morphology based on the Sloan Digital Sky Survey (SDSS), we obtain a sample of 66 irregular galaxies. We carry out new classification of them into GIGs and non-GIGs which have regular structure or show evidence for galaxy interaction, by using the SDSS Data Release 10 images. We then find that a half of these irregular galaxies (33/66) are GIGs and obtain an unambiguous sample of 33 GIGs for the first time. We discuss their observational properties by comparing them with those of elliptical, S0, spiral galaxies, and irregular galaxies without the GIGs. We find that our GIGs have smaller sizes, lower optical luminosities, bluer rest-frame optical colors, lower surface stellar mass densities, and lower gas metallicity than normal galaxies. All these properties suggest that they are in chemically and dynamically younger phases even in the nearby universe.

*Subject headings:* catalogs — galaxies: fundamental parameters — galaxies: photometry — galaxies: structure

### 1. INTRODUCTION

In the context of the hierarchical clustering scenarios for galaxy evolution, all galaxies in the present day are considered to acquire their masses by successive mergers of small building blocks of galaxies (e.g., White & Frenk 1991). Indeed, most galaxies observed in high-redshift universe are generally much smaller and much less massive than the present galaxies (Ferguson et al. 2004; van Dokkum et al. 2008; Taniguchi et al. 2009). Therefore, in order to understand the formation and early evolution of galaxies, it is necessary to explore which types of building blocks of galaxies were present and how the mass assembly process proceeded in the early universe.

Here a question arises as “are there any relics of such building blocks in the nearby universe?”. The best candidates are both gas-rich dwarf galaxies and irregular galaxies because these galaxies have a large amount of gaseous components even now<sup>7</sup> (e.g., Gallagher & Hunter 1984; Hunter & Gallagher 1986; Hunter et al. 2012). Therefore, in this paper, we focus on irregular galaxies as probable relic of building blocks of galaxies.

Since the galaxy morphology tells us dynamical properties of galaxies, morphological classifications of galaxies

provide us an important guideline in the understanding of galaxies. The most famous and pioneering work was made by Hubble (1926, 1936): the so-called Hubble classification of galaxy morphology. In his work, he stated that a few percent of galaxies do not show rotational symmetry and thus they cannot be classified in his classification scheme. They are called as irregular galaxies (Irr). He also stated that a half of irregular galaxies including Magellanic Clouds constitute an important population but the remaining galaxies are peculiar ones mostly due to galaxy interaction. Accordingly, irregular galaxies were recognized as heterogeneous populations (e.g., Sandage 1961).

Since irregular galaxies are minor populations, most studies have been devoted to the understanding of normal elliptical and spiral galaxies to date. Yet, irregular galaxies are important populations if they are not related to any galaxy interaction and mergers. Here we call them “genuine irregular galaxies (GIGs)” in this paper. GIGs are defined as isolated irregular galaxies without any regular structures (spheroid, bulge, disk, bar, spiral arm, and nucleus). In particular, we remind that the absence of nucleus is an important property, already noted by Hubble (1936). It is known that almost all ordinary galaxies have a galactic nucleus, that is believed to harbor a supermassive black hole (SMBH; Kormendy & Richstone 1995; Kormendy & Ho 2013 and references therein). The mass of SMBH is observed to be well correlated to that of the spheroidal component (bulge or spheroid) of galaxies (e.g. Magorrian et al. 1998; Kormendy & Ho 2013). Therefore the absence of nucleus implies that the spheroidal component has not yet developed in that galaxy.

It is thus suggested that irregular galaxies are still in an early evolutionary phase. This is also advocated by the presence of a plentiful amount of gas (e.g., Roberts & Hayes 1994; Hunter & Elmegreen 2004). Moreover, since irregular galaxies are less massive down to  $\sim 10^9 M_{\odot}$ ,

terao@cosmos.phys.sci.ehime-u.ac.jp

<sup>1</sup> Graduate School of Science and Engineering, Ehime University, Bunkyo-cho 2-5, Matsuyama, Ehime 790-8577, Japan

<sup>2</sup> Research Center for Space and Cosmic Evolution, Ehime University, Bunkyo-cho 2-5, Matsuyama, Ehime 790-8577, Japan

<sup>3</sup> Department of Particle and Astrophysical Science, Nagoya University, Furo-cho, Chikusa-ku, Nagoya 464-8602, Japan

<sup>4</sup> Department of Physics and Astronomy, Seoul National University, 599 Gwanak-ro, Gwanak-gu, Seoul 151-742, Korea

<sup>5</sup> Department of Astronomy, Kyoto University, Kitashirakawa-Oiwake-cho, Sakyo-ku, Kyoto 606-8502, Japan

<sup>6</sup> Research Fellow of the Japan Society for the Promotion of Science

<sup>7</sup> See the proceedings of IAU Symposium Vol.255, “Low Metallicity Star Formation: From the First Stars to Dwarf Galaxies” ed. L. K. Hunt, S. Madden, & R. Schneider (Cambridge: Cambridge Univ. Press)

we regard them as relics of building blocks of galaxies.

Motivated by this idea, we define GIGs, select a sample of GIGs, and then investigate their fundamental properties for the first time in this paper. Throughout this paper, magnitudes are given in the AB system. We adopt a flat universe with  $\Omega_M = 0.3$ ,  $\Omega_\Lambda = 0.7$ , and  $H_0 = 70 \text{ km s}^{-1} \text{ Mpc}^{-1}$ , throughout the paper.

## 2. GENUINE IRREGULAR GALAXIES

### 2.1. Definition

Originally, the class of irregular galaxies was defined by Hubble (1926), who investigated morphological properties of  $\sim 400$  galaxies in the nearby universe. He stated that; *About 3 per cent of the extra-galactic nebulae lack both dominating nuclei and rotational symmetry. These form a distinct class which can be termed "irregular". The Magellanic Clouds are the most conspicuous examples.* This definition is our guideline and, indeed, is the same as that of the GIGs discussed in this paper. The reason why we use the new term, GIG, is to exclude any contamination from the so-called peculiar galaxies mostly made by galaxy interactions and mergers (Hubble 1936). Such contamination also includes active galaxies with a superwind activity<sup>8</sup> (e.g., M82) and jets from an active galactic nucleus (e.g., M87).

To avoid any contamination, we re-define the class of GIGs as isolated galaxies without any regular structure. Here, the term of "isolated" means that there is no neighboring galaxy and there is no firm evidence for a recent galaxy merger. Note that the majority of ultraluminous infrared galaxies such as Arp 220 look isolated galaxies but they are major-merger remnants (e.g., Sanders & Mirabel 1996).

### 2.2. Samples

In order to obtain a well-defined sample of GIGs, we need reliable imaging survey for a large number of galaxies. We also need spectroscopic information to investigate their activity, metallicity, and physical sizes. One of the most suitable surveys for galaxies is the Sloan Digital Sky Survey (SDSS; York et al. 2000).

In fact, the following two excellent studies have been already made on morphological properties of galaxies:

1. Fukugita et al. (2007; hereafter F07)  
Based on the SDSS Data Release Three (DR3), they investigated 2253 galaxies with extinction-corrected  $r$  magnitude brighter than 16 mag in the north equatorial stripe (230 deg<sup>2</sup>). A total of 1866 galaxies also have spectroscopic information. In their analysis, irregular galaxies are termed as Im (i.e., Magellanic irregular). Among the 2253 galaxies, they identified 31 Im galaxies. This provides the fraction of irregular galaxies is  $\approx 1.4$  percent (= 31/2253).
2. Nair & Abraham (2010; hereafter NA10)  
Based on the SDSS Data Release Four (DR4), they investigated 14034 galaxies with extinction-corrected  $g$  magnitude brighter than 16 mag in all

SDSS fields (6670 deg<sup>2</sup>). All of their sample galaxies have spectroscopic information and lie in the redshift range,  $0.01 < z < 0.1$ . Among the 14034 galaxies, they identified 35 Im galaxies. This provides the fraction of irregular galaxies is  $\approx 0.25$  percent (= 35/14034). Note that NA10 also obtained 52 Sdm and 68 Sm galaxies in their analysis. However, since these galaxies show evidence for spiral arms, we use only 35 Im galaxies in the later discussion.

Then, we obtain 66 irregular galaxies (31 from F07 and 35 from NA10) in total. We list up these galaxies in Tables 1 (F07) and 2 (NA10), separately. These 66 galaxies are our preliminary sample of irregular galaxies.

It is noted that there is no overlap of Im galaxies between F07 and NA10 and the number fraction of the Im galaxies to the total galaxies is different with each other. This seems due to the following reasons. First, the data source is different between F07 (DR3) and NA10 (DR4). Second, the survey area of F07 is restricted to the north equatorial stripe (230 deg<sup>2</sup>), while that of NA10 is all SDSS fields (6670 deg<sup>2</sup>), which includes the survey area of F07. Third, the selection band is different:  $r \leq 16$  (F07) and  $g \leq 16$  (NA10). Fourth, NA10 uses a spectroscopic catalog and adopts the redshift criterion,  $0.01 < z < 0.1$ , while F07 uses a photometric catalog which includes the galaxies without spectroscopic information.

Much attention has been paid to dwarf irregular galaxies and very faint irregular galaxies because they can be more probable fossils of building blocks of galaxies (e.g., Hunter et al. 2012; Brown et al. 2013). However, we do not take absolute magnitudes into account in our sample selection because our main aim is to identify GIGs regardless of their luminosity.

### 2.3. Selection of GIGs

In order to identify unambiguous GIGs from the preliminary sample of 66 irregular galaxies, we examine their optical images carefully by using the SDSS Data Release Ten (DR10) database. Here we use the eye-inspection method. All the authors have examined individual galaxies and then have re-classified the preliminary sample into the following classes:

- (1) Elliptical-like galaxies:  
No object is found.
- (2) Disk-like galaxies:
  - (2-a) The presence of bulge with both spiral arms and a bar:  
No object is found.
  - (2-b) The presence of bulge with spiral arms and without bar:  
Four objects are found. Their color montages constructed by assigning RGB colors  $g$ ,  $r$ ,  $i$  data channels<sup>9</sup> are shown in Figure 1.
  - (2-c) The presence of bulge without spiral arms and with a bar:  
No object is found.

<sup>8</sup> These galaxies were once classified as Irr II (e.g., Sandage 1961).

<sup>9</sup> The images are taken from the SDSS Imaging Server: <http://skyserver.sdss3.org/dr10/en/tools/chart/navi.aspx>

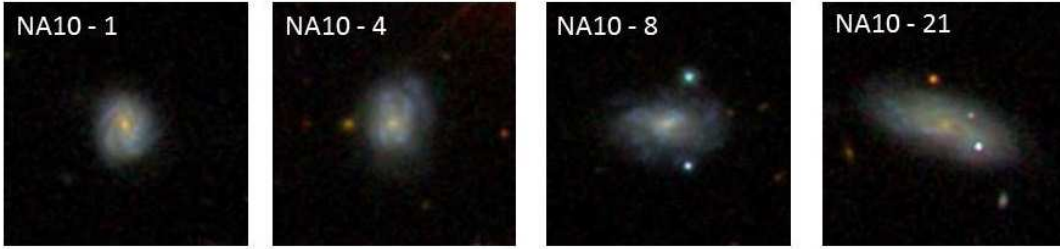


**Figure 1.** Montage of images of the 4 non-GIGs which are re-classified as disk with bulge and spiral arms and without a bar taken from the SDSS DR10. North is up and east is left. Image sizes are 60 arcsec  $\times$  60 arcsec.

- (2-d) The absence of bulge with both spiral arms and a bar:  
One object is found. Its image is shown in Figure 2.
- (2-e) The presence of bulge without both spiral arms and a bar:  
Six objects are found. Their images are shown in Figure 3.
- (2-f) The absence of bulge with spiral arms and without a bar:  
No object is found.
- (2-g) The absence of bulge without spiral arms and with a bar:  
No object is found.
- (3) The presence of a partner:  
Eight objects are found. Their images are shown in Figure 4. All these galaxies appear to be interacting galaxies. Comments on the individual galaxies are given in Appendix A.
- (4) Merger remnants:  
Fourteen objects are found. Their images are shown in Figure 5. All these galaxies appear to be merging galaxies. Comments on the individual galaxies are also given in Appendix A.
- (5) GIGs:  
Thirty three objects are found. Their images are shown in Figure 6. Although four objects (F07-22, F07-23, NA10-23, and NA10-29) seem to have companion in their images, they can be regarded as isolated as described in Appendix B.

We find that only 33 galaxies out of the 66 preliminary samples of irregular galaxies are re-classified into the unambiguous GIGs (22 from F07 and 11 from NA10). The remaining 33 galaxies are not GIGs (hereafter, non-GIGs). The sub-classes of the non-GIGs re-classified into (1), (2), (3), and (4) above are dubbed as non-GIG/E, non-GIG/Sp, non-GIG/I, and non-GIG/M, respectively. In Table 3, we summarize the statistics of the non-GIGs.

The redshifts are available for 28 GIGs (17 from F07 and 11 from NA10) among the 33 GIGs. The redshift information on F07-GIGs is taken from the SDSS DR10 database. However, it is noted that the redshift of one of the GIGs, F07-25, is given as 0.8124, which is extremely higher than the redshifts of the other F07-GIGs

with spectroscopic redshifts ( $z \sim 0.0032\text{--}0.027$ )<sup>10</sup>. Since its spectrum appears to be very noisy, we do not include this object in later discussion. Therefore our final spectroscopic sample consists of 27 GIGs (16 from F07 and 11 from NA10); hereafter we call them as zGIGs. We summarize the observational and physical information of the 33 GIGs including 27 zGIGs in Table 4.

We find that only a half of the preliminary samples of irregular galaxies are identified as unambiguous GIGs. Among the 33 non-GIGs, 33 percent (= 11/33) is re-classified into the disk-like galaxies (non-GIG/Sp) while the remaining 67 percent (= 22/33) is either interacting or merging galaxies (non-GIG/I+M). It is unclear whether or not there are any intrinsic differences between the non-GIGs and the GIGs. In order to answer the question, here we show comparisons of the  $g$ -band absolute magnitudes  $M_g$  and surface brightnesses  $\mu_g$  of the non-GIGs with redshift information (31 out of 33 non-GIGs) and the zGIGs.

#### 2.4. Comparison between GIGs and Non-GIG Samples

The zGIGs are fainter than the non-GIGs as clearly shown in the right-hand side cumulative histograms in the main panels of Figure 7. We also find that there is no GIGs with  $M_g \lesssim -20$  in both of F07 and NA10 samples. Among the very faint galaxies with  $M_g \gtrsim -17$ , which are available only in the F07 samples<sup>11</sup>, all galaxies except for a non-GIG, F07-30, are the zGIGs. Are these differences intrinsic one or merely a consequence of a kind of selection effect?

As shown in Figure 8, the cumulative histograms of  $\mu_g$  for the NA10-zGIGs and non-GIGs are similar with each other. Almost half of the F07-zGIGs (= 9/16) have  $\mu_g \lesssim 23.5$  mag arcsec<sup>-2</sup>, which is similar to the non-GIGs. Therefore, we can conclude that these zGIGs are bright enough to find any signatures of the presence of spiral arm, bar, and/or interaction/merger if exist. On the contrary, the remaining half of the F07-zGIGs (= 7/16) is fainter than 23.5 mag arcsec<sup>-2</sup>, which is comparable to that of the low surface brightness galaxies (LSBGs; e.g., Impey et al. 1996), although the GIGs do not have disk by definition. Hence, for these faint- $\mu_g$  zGIGs (from the faintest in  $\mu_g$ , F07-17, F07-21, F07-31, F07-9, F07-22, F07-19, and F07-20), it should be reminded there remains a possibility that they have signatures of

<sup>10</sup> If this redshift for F07-25 were correct, its absolute  $g$ -band magnitude  $M_g$  and size  $R_P$  would be estimated as  $M_g = -27.28$  and  $R_P = 156.6$  kpc, respectively.

<sup>11</sup> The selection criteria of  $m_g < 16$  and  $z > 0.01$  adopted in NA10 exclude these faint galaxies as shown in Figure 7.



**Figure 2.** Same as Figure 1 but for the 1 non-GIG which are re-classified as disk without bulge and with both spiral arm and a bar.

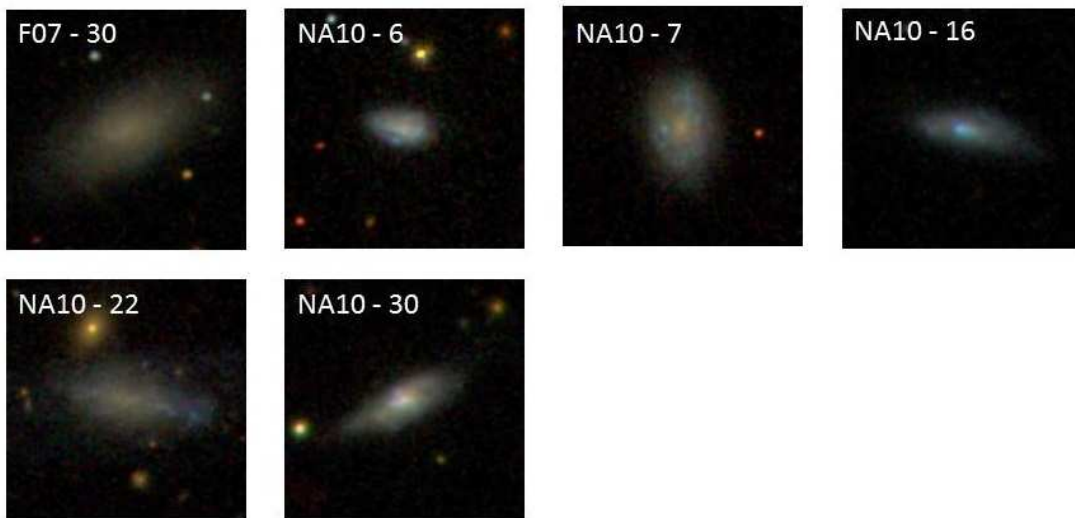


**Figure 3.** Same as Figure 1 but for the 6 non-GIGs which are re-classified as disk with bulge and without both spiral arm and a bar.

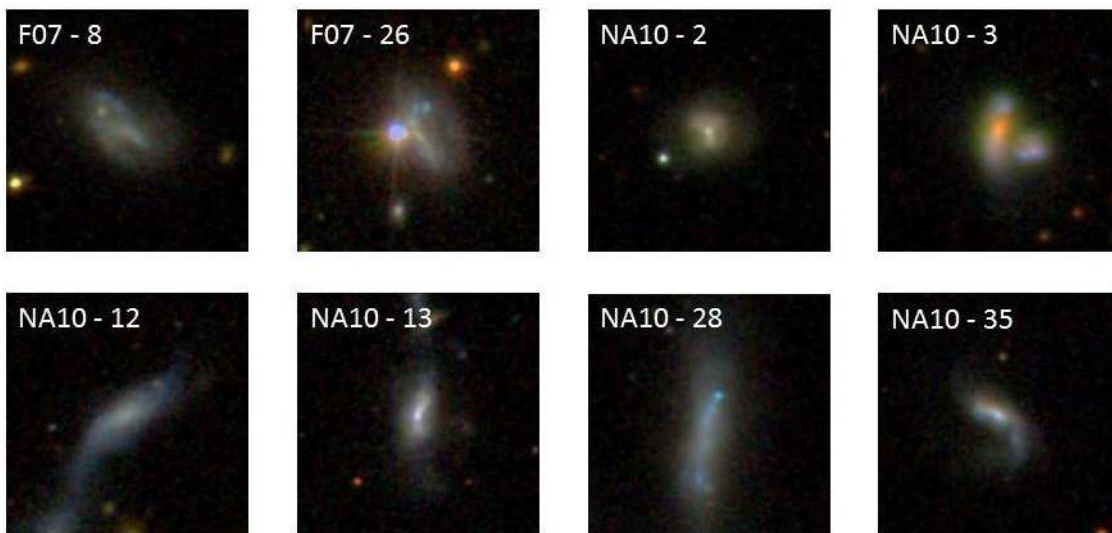


**Figure 4.** Same as Figure 1 but for the 8 non-GIGs which are re-classified as interacting galaxies, non-GIG/I.

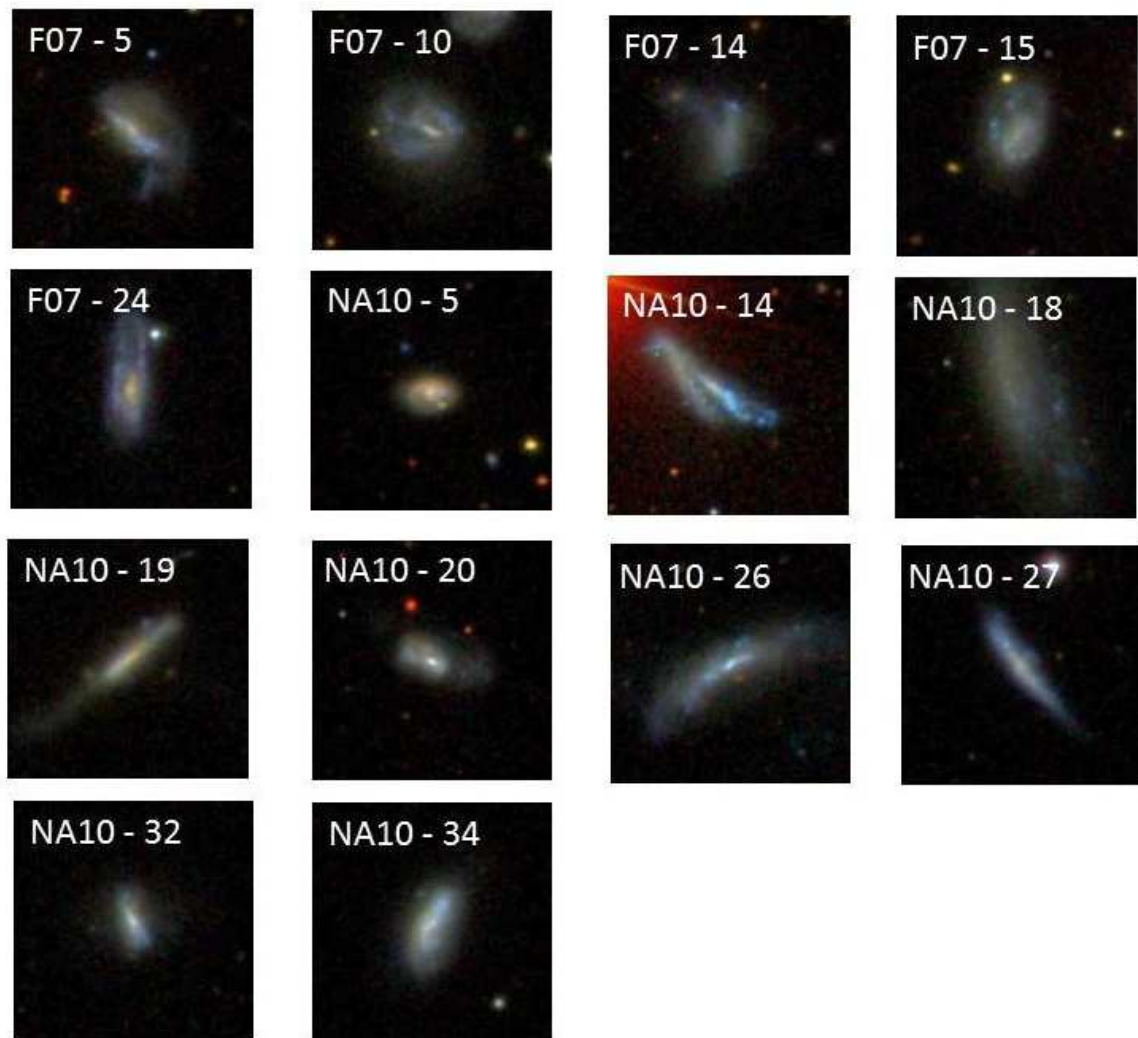


**Figure 5.** Same as Figure 1 but for the 14 non-GIGs which are re-classified as merging galaxies, non-GIG/M.

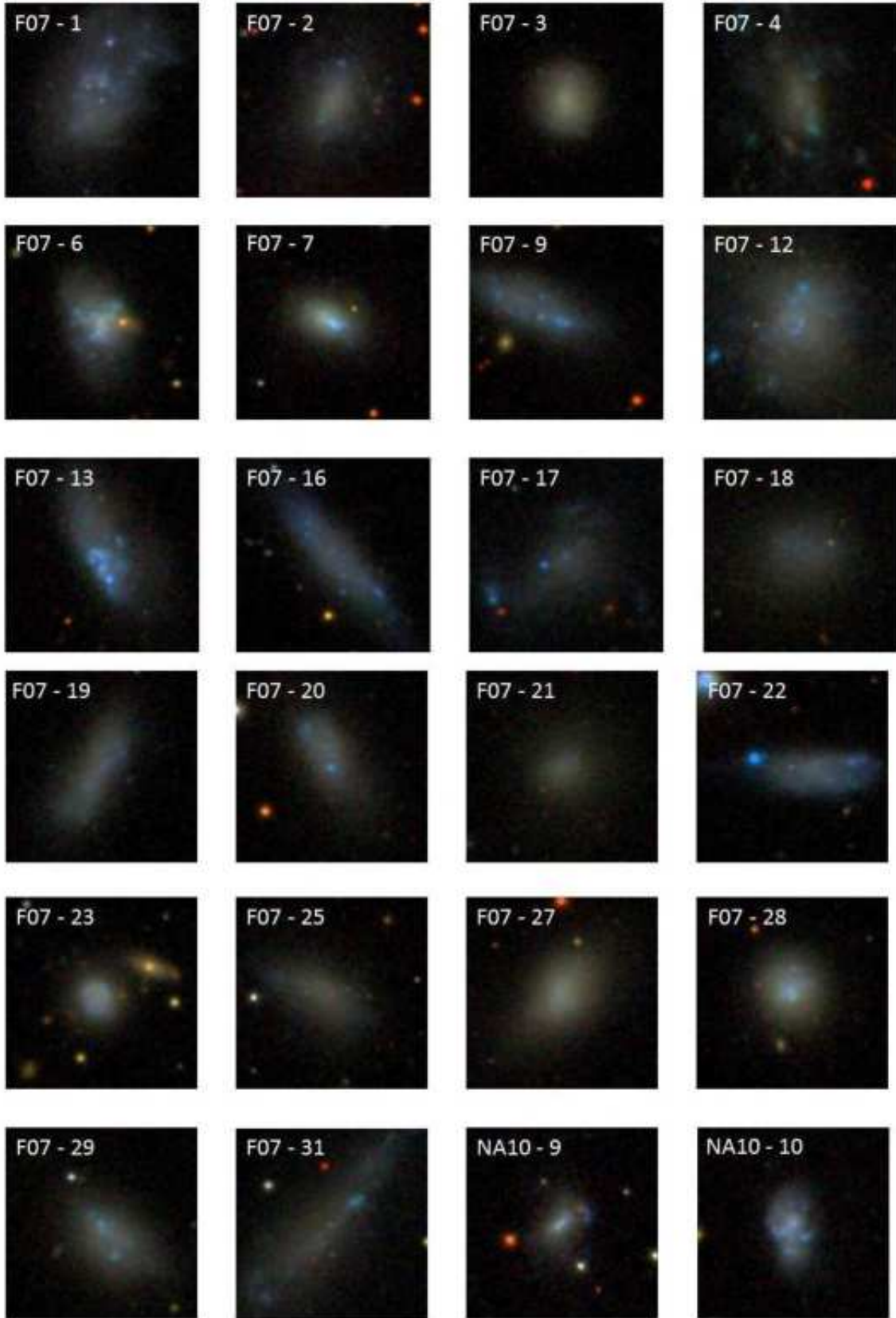
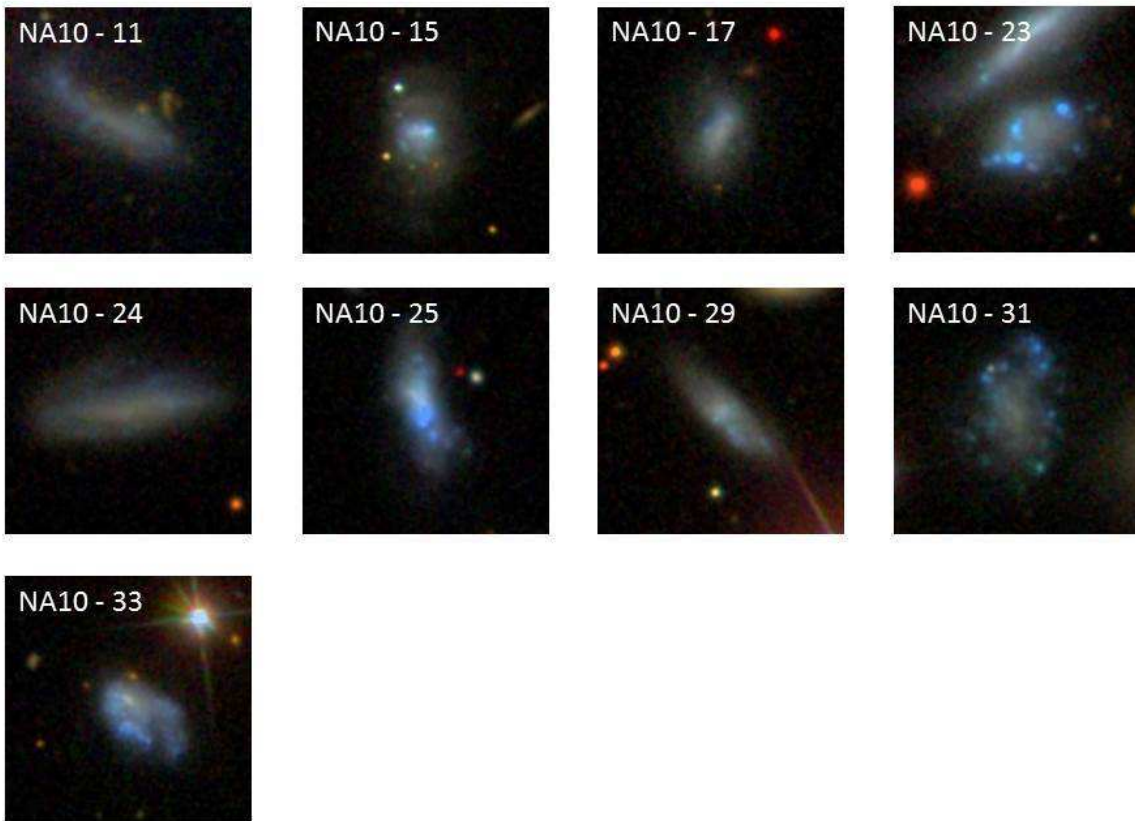


Figure 6. Same as Figure 1 but for the 33 GIGs.



**Figure 6.** (Continued.)

spiral arm, bar, and/or interaction/merger.

Including the GIGs without zGIGs, about 30 percent ( $= 10/33$ ) are so faint in  $g$ -band surface magnitude (i.e.,  $\mu_g > 23.5$  mag arcsec $^{-2}$ ) that we might miss any signatures of regular structure and/or interaction/merger. Nevertheless, the remaining 70% of the GIGs ( $= 23/33$ ) are sufficiently bright in  $\mu_g$  and hence they are regarded as unambiguous GIGs.

### 3. NATURE OF THE GIGS

In the previous section, we have newly defined the morphological class of GIGs as isolated galaxies without any regular structures. Then we selected a sample of 33 GIGs based on the two papers on the morphological classification of galaxies by using the SDSS data. Among the 33 GIGs, 27 have reliable redshift information, which are dubbed as zGIGs.

In this section, we investigate observational properties of the 27 zGIGs through comparisons with normal galaxies. As a control sample of normal galaxies that includes elliptical (E), S0, and spiral (Sp) galaxies, we use the SDSS galaxies studied by NA10 because all their galaxies have spectroscopic information and the sample number is significantly larger than that of F07. The total numbers of E/S0 and Sp galaxies are 5938 and 7708, respectively.

All the rest-frame photometric data for the NA10 galaxies are taken from Table 1 in NA10. The rest-frame photometry for F07 galaxies with redshift information is estimated by using the SDSS DR10 data with the  $k$ -correction following the procedure shown in Chilingarian & Zolotukhin (2012). Note also that all the photometric data are corrected for the Galactic extinction.

#### 3.1. $g$ -band Luminosity Function

We compare the number densities of the zGIGs to the control sample of normal galaxies and non-GIGs in order to examine whether or not the small detection number of the zGIGs implies intrinsically small number density. We show the luminosity functions (LF) of GIGs together with those of E/S0, Sp, and non-GIGs in Figure 9. The LFs are estimated by the so-called  $V_{\max}$  method (Schmidt 1968). Note, however, that the correction for the completeness is not made. The results are shown for the F07 and NA10 samples separately in Figure 9. In this Figure, the results are shown for the F07 and NA10 samples, separately.

First, we find that the LFs of GIGs show power-law like LFs for both the F07 and NA10 samples. Second, we find that the GIGs are the dominant population in fainter galaxies at  $M_g > -17$ . On the other hand, the fraction of GIGs is negligible ( $< 1\%$ ) at  $M_g < -19$ .

#### 3.2. Sizes and Absolute $g$ -band Magnitudes

We compare the physical size of zGIGs as a function of  $M_g$  with those of normal galaxies and the non-GIGs. Here, we use the Petrosian radius,  $R_P$ , as a size of galaxy. The results are shown in Figure 10. Compared to the control samples, the sizes of the zGIGs are significantly smaller. However, the  $R_P$ - $M_g$  relation for the GIGs appears to follow the same relation for the Sp sample.

The sizes of NA10-zGIGs (F07-zGIGs without F07-25 at  $z = 0.8$ ) are 3.28–6.01 kpc (1.06–2.20 kpc) with a median value of 3.82 kpc (1.68 kpc). We find that the

F07-zGIGs are systematically smaller than the NA10-zGIGs. This can be attributed to the fact that the F07-zGIGs are located at lower redshifts than the redshift threshold adopted in NA10 ( $z = 0.01$ ).

#### 3.3. Optical Colors

We compare the rest-frame optical color,  $(g - r)_0$ , of zGIGs with those of normal galaxies as a function of  $M_g$  in Figure 11. The zGIGs tend to be bluer than normal spiral galaxies on average and all the zGIGs are bluer than  $(g - r)_0 = 0.6$ . If the bluer color of zGIGs is attributed to recent massive star formation events, their star formation rate relative to the stellar mass (i.e., the specific star formation rate) is systematically higher than those of normal spiral galaxies (see Section 3.5).

#### 3.4. Stellar Mass Density

We compare the stellar mass density,  $\Sigma_*$ , of the zGIGs with normal galaxies as a function of  $M_g$  in Figure 12. The catalog of NA10 includes stellar mass estimated by Kauffmann et al. (2003a). For zGIGs in F07, we use the stellar mass in the same catalog. The GIGs tend to have lower stellar mass density compared to the Sp sample systematically. This suggests that the cumulative star formation rate in the GIGs is smaller than that of typical spiral galaxies.

#### 3.5. Ionization Sources

All the 27 zGIGs show strong optical emission lines. In order to study major ionization sources in them, we use the so called excitation diagram between  $[\text{N II}]\lambda 6584/\text{H}\alpha$  and  $[\text{O III}]\lambda 5007/\text{H}\beta$  emission line ratios (e.g., Baldwin, Phillips, & Terlevich 1981; Veilleux & Osterbrock 1987). Since the GIGs have no nucleus by definition, there is no contribution from active galactic nuclei. It is therefore expected that most probable ionization sources are massive OB stars. In fact, we find that all the zGIGs show H II-region like properties in Figure 13. Here, the emission line flux data are taken from the SDSS DR10 database. Note that the two GIGs, F07-7 (SDSS J105248.63+000203.9) and F07-22 (SDSS J131743.19 – 010003.8), show strong  $\text{H}\beta$  absorption. Since this makes difficult to estimate their  $\text{H}\beta$  emission, we show these data points as upper limits in Figure 13.

We then conclude that the major ionization sources in the zGIGs are massive OB stars. If the superwind activity works effectively, ionization would be dominated by shock heating. If this is the case, the zGIGs would be located around  $[\text{N II}]\lambda 6584/\text{H}\alpha \sim 0$  (e.g., Veilleux & Osterbrock 1987). Therefore, it is suggested that the superwind activity is fairly low in the zGIGs.

Finally, it should be mentioned that the majority of zGIGs are located in a domain with both  $[\text{N II}]\lambda 6584/\text{H}\alpha < -1$  and  $[\text{O III}]\lambda 5007/\text{H}\beta > 0$  in Figure 13. This implies that the zGIGs are metal poor galaxies (e.g., Kewley et al. 2001). In fact, typical nuclear starburst galaxies are located in a domain with both  $[\text{N II}]\lambda 6584/\text{H}\alpha \sim -0.5$  and  $[\text{O III}]\lambda 5007/\text{H}\beta < 0.5$  (Balzano 1983; Ho et al. 1997; Kauffmann et al. 2003b). Based on the theoretical study by Kewley et al. (2001), it is suggested that the gas metallicity of zGIGs range from  $0.5 Z_\odot$  to  $1 Z_\odot$  (see next section).



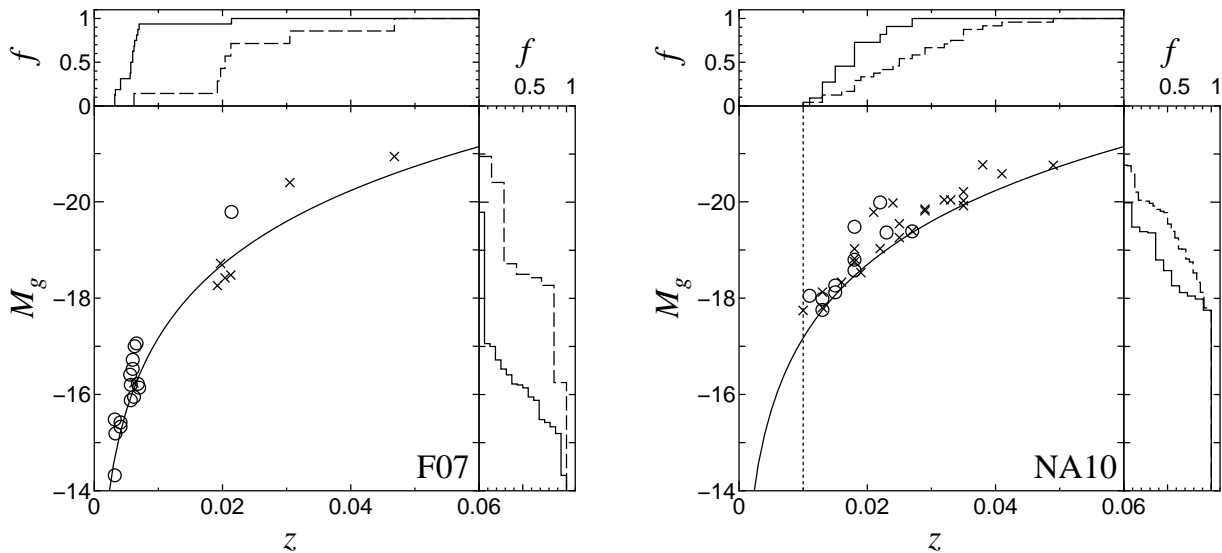


**Figure 7.** A comparison of the  $g$ -band absolute magnitude  $M_g$  and redshift distributions for F07 (left) and NA10 (right). In the main panels, the zGIGs and non-GIGs are represented by the open circles and the crosses, respectively. The solid curves present a constant  $g$ -band magnitude,  $m_g = 16$ , which is the selection criterion in NA10. The vertical dotted-line in the right main panel is the threshold redshift adopted in NA10,  $z = 0.01$ . The plot in the main panel is projected onto the two side panels where a cumulative histogram is displayed for each population in each of the dimensions. In the two sub-panels, the zGIGs and non-GIGs are shown by the solid and dashed histograms, respectively.

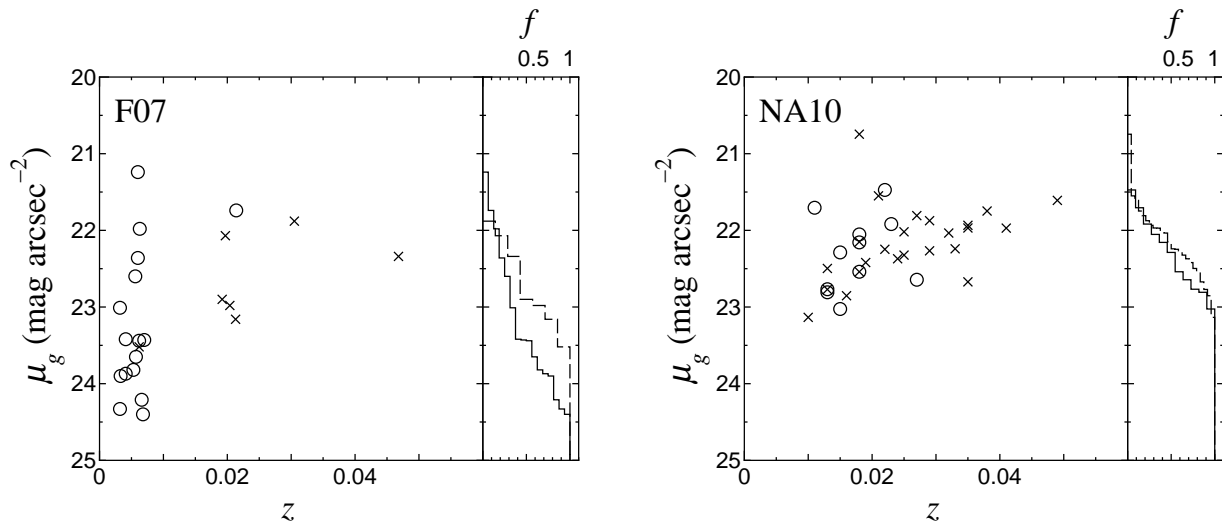


**Figure 8.** Same as Figure 7 but for  $g$ -band surface brightness  $\mu_g$  and redshift distributions for F07 (left) and NA10 (right).

### 3.6. Gas Metallicity

Optical emission-line ratios are also used to estimate the gas metallicity of galaxies (e.g., Kewley & Ellison 2008 and references therein). In the estimate of gas metallicity, the so-called  $R_{23}$  parameter has been often used:  $R_{23} = ([\text{O II}]\lambda 3727 + [\text{O III}]\lambda 4959, 5007)/\text{H}\beta$ . However, the  $[\text{O II}]\lambda 3727$  is outside of the SDSS spectral coverage for most nearby galaxies. Since it has been shown that the  $N2$  parameter,  $N2 = \log([\text{N II}]\lambda 6584/\text{H}\alpha)$ , also works well for the estimate of gas metallicity (e.g., Denicoló et al. 2002; Pettini & Pagel 2004), we use the  $N2$  parameter in our analysis. We use the following  $N2$  calibration formula obtained by Pettini & Pagel (2004):

$$12 + \log(\text{O}/\text{H}) = 8.90 + 0.57 \times N2. \quad (1)$$

The gas metallicity obtained from this formula is given in the last column of Table 3. The gas metallicity ranges from 8.08 to 8.81 with the median value of 8.31. Here we note that the gas metallicity of F07-21, 8.81, appears to be unusually high for its absolute magnitude,  $M_g = -14.32$ . Since its optical spectrum shows very strong  $\text{H}\beta$  absorption, the  $\text{H}\alpha$  emission flux could be underestimated significantly. In order to estimate its gas metallicity unambiguously, we need new detailed optical spectroscopy for this object. It is also encouraged to use other metallicity indicators, such as  $R_{23}$ , for future investigations because there is a possible systematic difference of the estimated gas metallicity from  $R_{23}$  and  $N2$  parameters,  $\sim 0.3$  dex (e.g., Cullen et al. 2013).

In Figure 14, we show the gas metallicity to the abso-

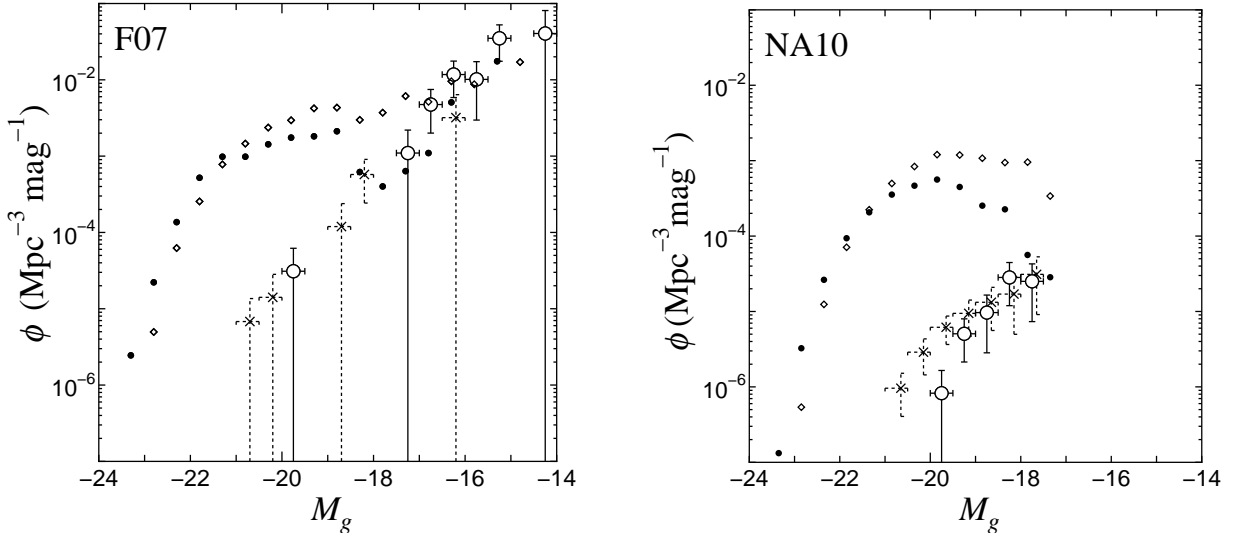


**Figure 9.** The  $g$ -band luminosity functions for F07 (left) and NA10 (right) GIGs. The  $g$ -band luminosity functions of GIGs, non-GIGs, E/S0, and spiral (Sp) galaxies are shown by open circles, crosses, small filled circles, and small open diamonds, respectively. The  $1\sigma$  Poissonian errors of the number densities are presented as vertical error-bars only for the GIGs and non-GIGs because of their small numbers. To avoid an overlap of symbols, the symbols of E/S0 galaxies, spiral galaxies, and non-GIGs are shifted horizontally by  $-0.1$ ,  $0$ , and  $+0.1$  mag, respectively.

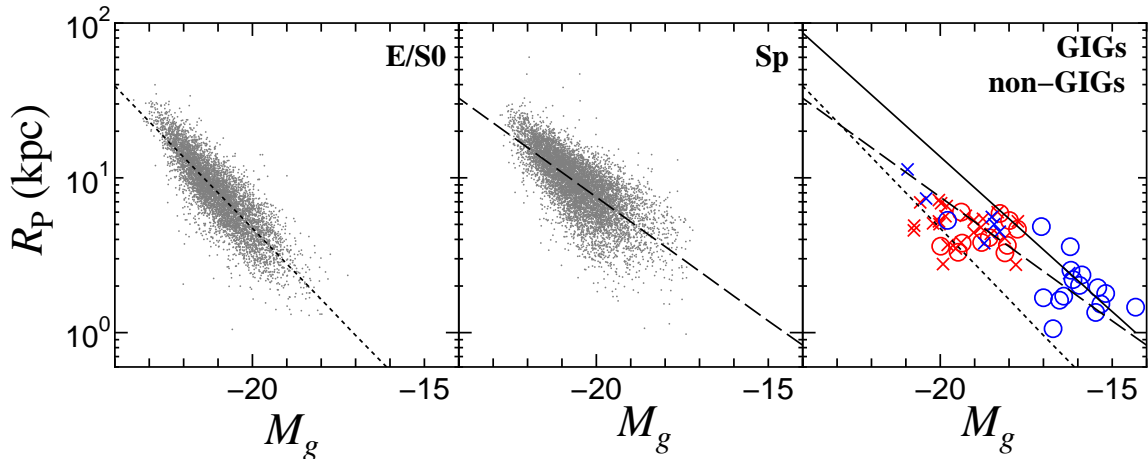


**Figure 10.** Diagrams between the size  $R_P$  and the  $g$ -band absolute magnitude  $M_g$  for E/S0 (left), Sp (middle), and zGIGs and non-GIGs with redshift information (right). The regression lines for E/S0 and Sp are shown by the dotted and dashed lines, respectively. These lines are also shown in the right panel for reference. In the right panel, blue and red symbols are for the F07 and NA10 samples, respectively. A locus of constant  $g$ -band surface brightness of  $\mu_g = 23.5$  mag arcsec $^{-2}$  is also shown by solid line for reference.

lute  $g$ -band magnitude relation between the zGIG and the star-forming galaxies in the NA10 catalog. The metallicities of both samples are evaluated from  $N2$  parameter. For the star-forming galaxies in NA10, we use galaxies in which both  $H\alpha$  and  $[N II]\lambda 6584$  are detected in high significance ( $S/N > 3$ ). We also show the contours that enclose 68% and 95% of the star-forming galaxies as solid lines and dashed lines. All zGIGs but F07-21 appear to be systematically metal poorer than the star-forming galaxies in NA10. It is also noted that the gas metallicity of our zGIGs is lower than the solar metallicity,  $12 + \log(O/H) = 8.66$  (Asplund et al. 2005), if we exclude F07-21.

#### 4. CONCLUSION

In this paper, we have defined the class of genuine irregular galaxies (GIGs) and selected a sample of 33 GIGs

from literature. This sample is not a complete one in any sense. Our main purpose is to unambiguously pick up irregular galaxies originally defined by Hubble (1926). As noted by Hubble (1936), a half of irregular galaxies are contaminations from interacting/merging galaxies and starburst galaxies and galaxies with an AGN. In fact, our analysis shows that 33 irregular galaxies among the 66 ones are not genuine irregular galaxies. It is thus suggested that  $\sim 50$  percent of irregular galaxies in previous statistical studies on galaxy morphology are not GIGs and thus statistical properties of irregular galaxies are affected by this selection bias.

More importantly, if we have a reliable sample of GIGs in the nearby universe, we are able to examine their observational properties and then obtain some observational clues in the understanding of building blocks of galaxies. In fact, our GIGs have smaller physical sizes

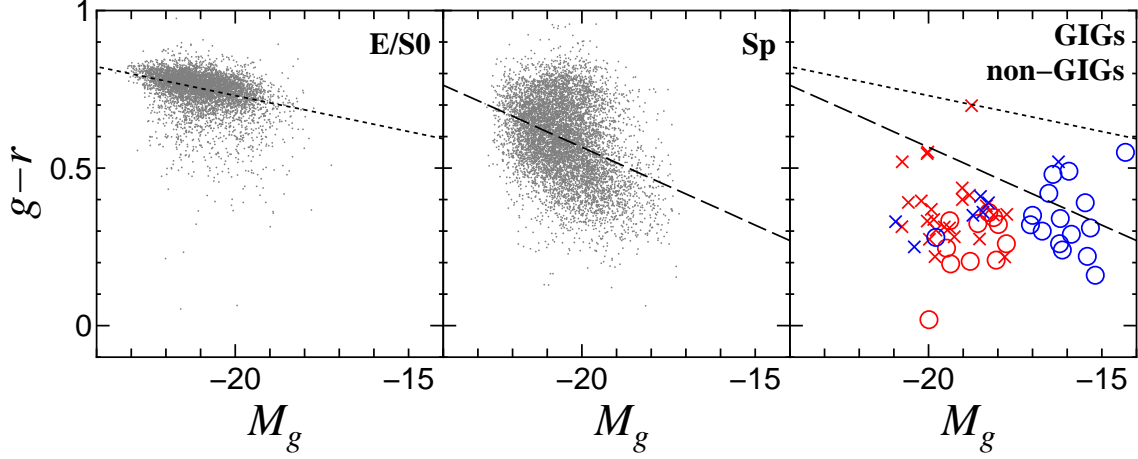


**Figure 11.** Same as Figure 10 but for the rest-frame  $g-r$  color and the  $g$ -band absolute magnitude.

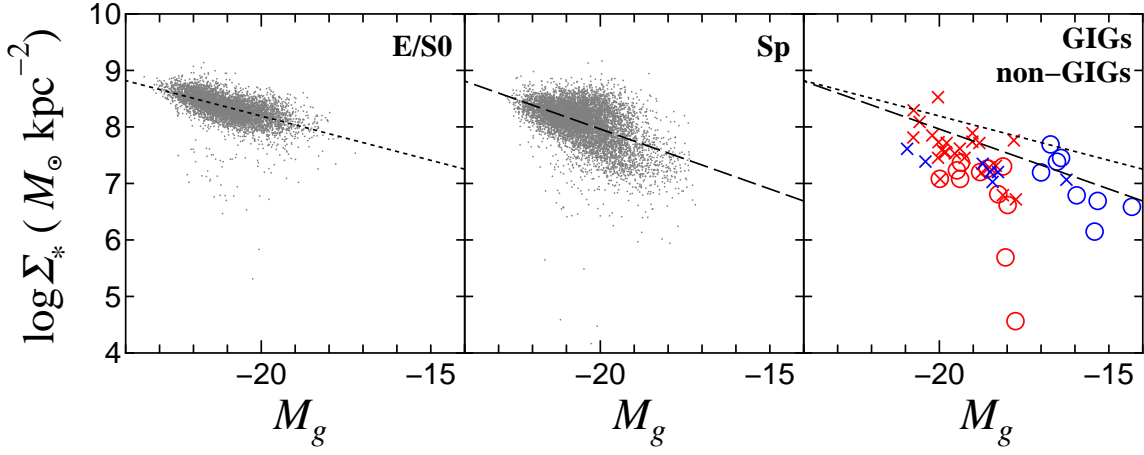


**Figure 12.** Same as Figure 10 but for the surface mass density  $\Sigma_*$  and the  $g$ -band absolute magnitude

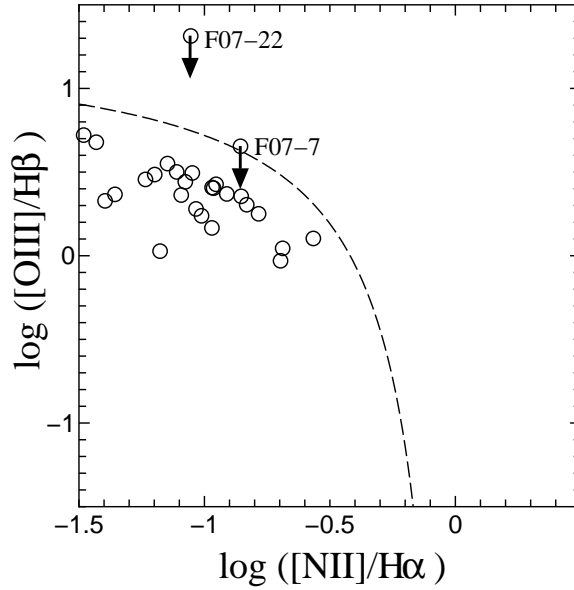


**Figure 13.** Diagram between  $[\text{N II}]\lambda 6584/\text{H}\alpha$  and  $[\text{O III}]\lambda 5007/\text{H}\beta$  for the 27 zGIGs, for which optical spectra are available in the SDSS data archive. The dashed curve shows the border between H II region and AGN excitation taken from Kauffmann et al. (2003b). For the two objects, F07-7 (SDSS J105248.63 + 000203.9) and F07-22 (SDSS J131743.19 - 010003.8), the upper limits of the  $[\text{O III}]\lambda 5007/\text{H}\beta$  ratio are shown because strong  $\text{H}\beta$  absorption appears in their spectra. It is thus considered that the apparent very high  $[\text{O III}]\lambda 5007/\text{H}\beta$  ratio is due to the underestimate of  $\text{H}\beta$  emission.

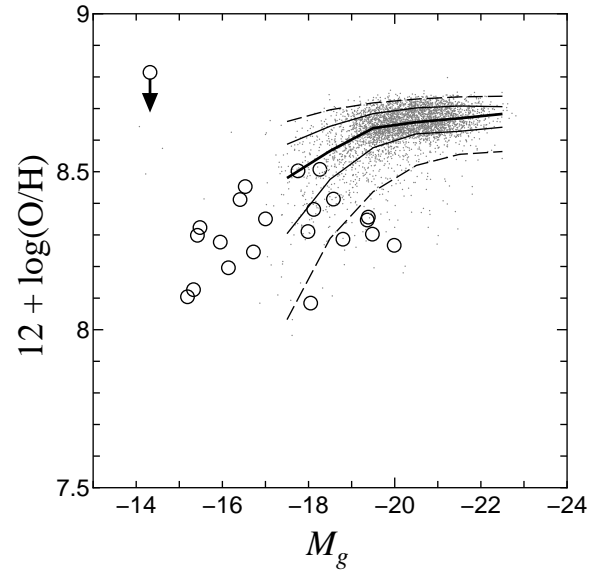


**Figure 14.** Comparison of gas metallicity derived from the N2 index given in equation (1) as a function of  $g$ -band absolute magnitude between the zGIGs and star-forming galaxies in NA10. The zGIGs are represented by the open circles, while the SDSS star-forming galaxies are shown by dots. The solid and dashed curves enclose 68% and 95% of them, respectively.

and absolute luminosities than those of normal galaxies. Also, they have no evidence for the bulge component. This suggests that an SMBH is not present even now since we cannot find their galactic nucleus. Furthermore, since the GIGs have lower metallicity than that of normal galaxies, they are in younger stages in the context of chemical evolution of galaxies.

In conclusion, it is important to make systematic studies of GIGs, providing us what happened in the early evolution of galaxies at high redshift universe. Our future plans are the followings. (1) We will make our own systematic surveys of GIGs using archival imaging data obtained with the Suprime-Cam on the 8.2 m Subaru Telescope. Our main target fields are the SDF (Kashikawa

et al. 2004), SXDS (Furusawa et al. 2008) and COSMOS (Scoville et al. 2007; Taniguchi et al. 2007). (2) In this paper, we have realized that eye-ball classification of galaxy morphology is basically a hard business. This means that we need an automated and more sophisticated classification scheme of GIGs. We will prepare this type of software and then apply it to future studies of galaxy morphology.

We would like to thank Takashi Murayama for useful discussion. This work was financially supported in part by the Japan Society for the Promotion of Science (JSPS; No.23244031 [YT] and No. 23740152 [MK]). HI is financially supported by the JSPS through the JSPS Research Fellowship.

## APPENDIX

### A. COMMENTS ON EACH GALAXY RE-CLASSIFIED INTO THE NON-GIGS/I+M

Here we provide comments on the irregular galaxies in the preliminary samples identified as either interacting or merging galaxies in our classification.

#### 1. Interacting galaxies

**F07-8:** An asymmetric structure is seen in NE.

**F07-26:** This object is regarded as a ring galaxy (Theys & Spiegel 1976; Toomre & Toomre 1972). A probable colliding partner is a small galaxy seen at SSE.

**NA10-2:** Weak but asymmetric feature can be seen. A small galaxy seen at NEE may be an interacting partner.

**NA10-3:** An interacting partner can be seen at W.

**NA10-12:** The overall structure is highly asymmetric. An interacting partner is located at SSE.

**NA10-13:** The overall structure is asymmetric. An interacting partner is located at N.

**NA10-28:** The overall structure is asymmetric. An interacting partner is located at S.

**NA10-35:** The overall structure is asymmetric. An interacting partner is located at SW.

#### 2. Merging galaxies

**F07-5:** One-sided arm can be seen at N. This structure may take an polar orbit, being similar to Arp 336 (NGC 2685; Arp 1966). A small object located at S may be a merging partner or its relic.

**F07-10:** The overall structure is highly asymmetric, evidenced by extended structure at E.

**F07-14:** One-sided structure is emanated from the southern part of the main body. This can be regarded as a tidal tail.

**F07-15:** One-sided structure is emanated from the NW part of the main body. This can be regarded as a tidal tail.

**F07-24:** One-sided structure is emanated from the northern part of the main body. This can be regarded as a tidal tail.

**NA10-5:** One-sided structure is emanated from the eastern part of the main body. This can be regarded as a tidal tail.

**NA10-14:** One-sided structure is emanated from the NE part of the main body. This can be regarded as a tidal tail.

**NA10-18:** The overall structure is asymmetric, evidenced by extended structure toward N.

**NA10-19:** One-sided structure is emanated from the SE part of the main body. This can be regarded as a tidal tail seen from the edge-on.

**NA10-20:** The overall structure is highly asymmetric, evidenced by small (at E) and large (W) plume-like structures.

**NA10-26:** The overall structure shows significant bending.

**NA10-27:** The overall structure shows significant bending.

**NA10-32:** The overall structure shows an integral-like pattern.

**NA10-34:** The overall structure shows an inverse integral-like pattern. The small knot located at the NNW edge may be a merging partner.

**Table 1**  
A list of 31 irregular galaxies in F07.

Name		Observed Magnitude		$\mu_g$ (mag arcsec <sup>-2</sup> )	Our Class <sup>a</sup>
Ours	F07	<i>g</i>	<i>r</i>		
F07-1	22	15.47	15.23	23.00	GIG
F07-2	26	16.14	15.78	23.42	(z)GIG
F07-3	41	15.96	15.44	22.36	(z)GIG
F07-4	45	16.79	16.14	23.44	(z)GIG
F07-5	47	15.80	15.41	21.88	non-GIG/M
F07-6	402	15.25	14.91	21.74	(z)GIG
F07-7	596	15.51	15.17	21.24	(z)GIG
F07-8	658	16.55	16.09	23.16	non-GIG/I
F07-9	709	15.70	15.50	23.90	(z)GIG
F07-10	744	15.98	15.61	22.11	non-GIG/M
F07-11	773	16.50	16.08	22.90	non-GIG/Sp
F07-12	861	15.32	14.91	23.01	(z)GIG
F07-13	952	15.93	15.82	23.27	GIG
F07-14	1030	16.41	16.04	22.98	non-GIG/M
F07-15	1046	16.04	15.68	22.07	non-GIG/M
F07-16	1114	15.92	15.71	23.94	GIG
F07-17	1128	16.20	15.91	24.40	(z)GIG
F07-18	1139	16.49	15.93	23.68	GIG
F07-19	1193	16.02	15.70	23.82	(z)GIG
F07-20	1196	15.82	15.46	23.65	(z)GIG
F07-21	1281	16.46	15.88	24.33	(z)GIG
F07-22	1404	15.93	15.69	23.87	(z)GIG
F07-23	1433	16.19	15.74	22.23	GIG
F07-24	1532	15.76	15.41	22.34	non-GIG/M
F07-25	1896	16.42	15.79	24.09	GIG <sup>b</sup>
F07-26	1903	15.90	15.67	22.39	non-GIG/I
F07-27	1908	15.62	15.11	22.60	(z)GIG
F07-28	1984	15.41	15.00	21.98	(z)GIG
F07-29	2002	16.45	16.17	23.43	(z)GIG
F07-30	2074	16.05	15.48	23.52	non-GIG/Sp
F07-31	2244	15.61	15.18	24.21	(z)GIG

**Note.** — (a) GIG and non-GIG are genuine irregular galaxies and not GIG, respectively. zGIG is the GIG with spectroscopic redshift. For sub-classes of the non-GIG, see Table 3. (b) Although F07-25 have spectroscopic information, we do not include this object in our zGIG sample since the spectrum appears to be very noisy (see footnote 11).

## B. COMMENTS ON THE GIGS WITH APPARENT COMPANION

Here we give comments on the following four GIGs with apparent companion in their images shown in Figure 6: F07-22, F07-23, NA10-23, and NA10-29.

**F07-22:** The object at the NE edge of the image in Figure 6 is classified as a star in the SDSS DR10.

**F07-23:** The yellow extended object at NW of the F07-23 is a galaxy at  $z = 0.11$ . Although F07-23 does not have spectroscopic information, it may be located at a similar redshift with the F07-zGIGs ( $= 0.0032\text{--}0.027$ ), which is much smaller than that of the NW galaxy. Note that no signature of interaction is seen in the NW galaxy albeit its relatively high surface brightness.

**NA10-23:** There is a large blue extended object at N of NA10-23. It is classified as a galaxy in the SDSS DR10 and does not have a spectroscopic information. Its photometric redshift is highly uncertain and includes the redshift of NA10-23 ( $= 0.011$ ) within  $1\sigma$  error. However, no signature of interaction is seen in the N galaxy albeit its relatively high surface brightness ( $= 21.75$  mag arcsec<sup>-2</sup>).

**NA10-29:** The yellow extended object at NNW of the NA10-29 is classified as a galaxy in the SDSS DR10. Although it does not have spectroscopic information, its photometric redshift is provided as  $\approx 0.06$ , which is much larger than the redshift of NA10-29 ( $= 0.015$ ).

## REFERENCES

- Arp, H. 1966, Atlas of Peculiar Galaxies (Pasadena, CA: California Institute of Technology)  
 Asplund, M., Grevesse, N., & Sauval, A. J. 2005, Cosmic Abundances as Records of Stellar Evolution and Nucleosynthesis, 336, 25  
 Baldwin, J. A., Phillips, M. M., & Terlevich, R. 1981, PASP, 93, 5  
 Balzano, V. A. 1983, ApJ, 268, 602

**Table 2**  
A list of 35 irregular galaxies in NA10.

Ours	Name	Observed Magnitude		$\mu_g$ (mag arcsec <sup>-2</sup> )	Our Class <sup>a</sup>
	NA10	$g$	$r$		
NA10-1	J120301.00-001728.21	15.91	15.41	21.97	non-GIG/Sp
NA10-2	J142911.77-001415.25	16.05	15.51	22.67	non-GIG/I
NA10-3	J142227.61+000332.68	15.98	15.16	22.04	non-GIG/I
NA10-4	J114359.62+002540.84	15.92	15.51	22.27	non-GIG/Sp
NA10-5	J135942.73+010637.28	16.15	15.62	21.61	non-GIG/M
NA10-6	J014836.90+124222.07	16.24	15.87	21.81	non-GIG/Sp
NA10-7	J003234.97+150210.45	15.94	15.43	22.54	non-GIG/Sp
NA10-8	J114242.96-022138.61	15.93	15.60	22.32	non-GIG/Sp
NA10-9	J085111.80+543958.32	15.96	15.68	22.64	(z)GIG
NA10-10	J123012.10+033439.88	15.68	15.48	22.16	(z)GIG
NA10-11	J021121.62-100715.77	15.89	15.57	22.81	(z)GIG
NA10-12	J020238.79-092213.39	16.05	15.76	22.42	non-GIG/I
NA10-13	J225609.41+130551.47	15.50	15.22	21.75	non-GIG/I
NA10-14	J211444.78+105221.37	16.06	15.69	20.75	non-GIG/M
NA10-15	J223921.86+135256.22	15.62	15.39	22.05	(z)GIG
NA10-16	J110037.12+040355.07	15.99	15.77	22.50	non-GIG/Sp
NA10-17	J233225.26-005049.28	15.98	15.67	22.54	(z)GIG
NA10-18	J024421.10+004031.16	16.18	15.81	23.14	non-GIG/M
NA10-19	J114710.16+103103.63	15.99	15.53	22.25	non-GIG/M
NA10-20	J162734.31+390604.06	16.07	15.72	21.97	non-GIG/M
NA10-21	J014230.89-004909.99	15.56	15.08	22.15	non-GIG/Sp
NA10-22	J223436.81+001024.37	15.97	15.46	22.85	non-GIG/Sp
NA10-23	J090015.20+354319.73	16.48	16.46	21.71	(z)GIG
NA10-24	J092938.47+352025.26	15.70	15.30	23.03	(z)GIG
NA10-25	J110508.10+444447.09	14.72	14.73	21.47	(z)GIG
NA10-26	J121725.85+463400.88	15.02	14.79	22.37	non-GIG/M
NA10-27	J131055.81+115229.20	15.82	15.57	21.87	non-GIG/M
NA10-28	J140056.40+410025.92	15.64	15.33	22.77	non-GIG/I
NA10-29	J132852.21+110549.21	15.92	15.56	22.29	(z)GIG
NA10-30	J113655.36+115054.03	15.51	15.08	21.93	non-GIG/Sp
NA10-31	J114830.62+124347.08	19.50	19.25	22.77	(z)GIG
NA10-32	J132032.98+124922.57	15.76	15.42	22.02	non-GIG/M
NA10-33	J140156.73+122249.78	15.78	15.57	21.92	(z)GIG
NA10-34	J131606.19+413004.24	15.06	14.73	21.55	non-GIG/M
NA10-35	J102722.42+121701.36	16.04	15.73	22.24	non-GIG/I

**Note.** — (a) GIG and non-GIG are genuine irregular galaxies and not GIG, respectively. zGIG is the GIG with spectroscopic redshift. For sub-classes of the non-GIG, see Table 3.

**Table 3**  
A list of non-GIGs.

	Contaminant	Number			Details	Sub-class Name					
		Total	F07	NA10							
(1)	Elliptical-like galaxies	0	0	0		non-GIG/E					
(2)	Disk-like galaxies	11	2	9		non-GIG/Sp					
					Bulge	Spiral Arm	Bar	Number			
								Total	F07	NA10	
					(2-a)	○	○	○	0	0	0
					(2-b)	○	○	×	4	0	4
					(2-c)	○	×	○	0	0	0
					(2-d)	×	○	○	1	1	0
					(2-e)	○	×	×	6	1	5
					(2-f)	×	○	×	0	0	0
					(2-g)	×	×	○	0	0	0
(3)	Interacting galaxies	8	2	6							non-GIG/I
(4)	Merging remnants	14	5	9							non-GIG/M
	Total	33	9	24							

**Table 4**  
A list of 33 GIGs including 27 zGIGs.

Ours	Name SDSS	$z$	$R_p$ (kpc)	$M_g^a$ (mag)	$\mu_g^a$ (mag arcsec $^{-2}$ )	$(g-r)_0^a$ (mag)	$12 + \log(O/H)$
F07: 22 GIGs including 16 zGIGs							
F07-1	J094407.21-003935.3	...	...	...	23.00	...	...
F07-2	J094446.23-004118.2	0.0041	1.53	-15.33	23.42	0.30	8.13
F07-3	J094628.56-002603.4	0.0060	1.62	-16.53	22.36	0.41	8.45
F07-4	J094705.49+005751.2	0.0062	2.02	-15.95	23.44	0.49	8.28
F07-6	J102519.78+003810.4	0.0214	5.43	-19.79	21.74	0.28	8.62
F07-7	J105248.63+000203.9	0.0060	1.06	-16.72	21.24	0.29	8.25
F07-9	J111054.18+010530.5	0.0033	1.79	-15.19	23.90	0.16	8.10
F07-12	J112712.26-005940.7	0.0032	1.35	-15.48	23.01	0.39	8.32
F07-13	J115036.31-003403.0	...	...	...	23.27	...	...
F07-16	J122021.40+002204.2	...	...	...	23.94	...	...
F07-17	J122412.46+003401.9	0.0068	3.59	-16.22	24.40	0.26	8.06
F07-18	J122903.25+000616.9	...	...	...	23.68	...	...
F07-19	J124002.65-010257.6	0.057	2.36	-15.88	23.82	0.29	8.22
F07-20	J124008.77-002107.7	0.066	4.84	-16.20	23.65	0.34	8.35
F07-21	J125405.16-000604.3	0.0032	1.46	-14.32	24.33	0.55	8.81
F07-22	J131743.19-010003.8	0.0041	1.95	-15.42	23.87	0.21	8.30
F07-23	J132009.17-011128.3	...	...	...	22.23	...	...
F07-25	J144300.18-002300.2	(0.8124) <sup>b</sup>	(156.6)	(-27.28)	24.09	...	...
F07-27	J144515.80-000934.3	0.0056	1.72	-16.41	22.60	0.47	8.41
F07-28	J150001.30-010527.8	0.0063	1.68	-17.00	21.98	0.34	8.35
F07-29	J150350.19+005841.8	0.0070	2.20	-16.14	23.43	0.23	8.20
F07-31	J154219.30+002831.3	0.0066	4.84	-17.06	24.21	0.32	8.22
NA10: 11 GIGs including 11 zGIGs							
NA10-9	J085111.76+543958.3	0.027	6.01	-19.39	22.64	0.33	8.36
NA10-10	J123012.10+033439.9	0.018	3.82	-18.80	22.16	0.20	8.29
NA10-11	J021121.60-100716.3	0.013	5.30	-17.99	22.81	0.32	8.31
NA10-15	J223922.29+135300.2	0.018	3.30	-19.48	22.05	0.25	8.30
NA10-17	J233225.25-005049.1	0.018	4.11	-18.58	22.54	0.32	8.41
NA10-23	J090015.20+354319.7	0.011	3.66	-18.05	21.71	0.21	8.08
NA10-24	J092938.46+352025.2	0.015	5.89	-18.26	23.03	0.36	8.51
NA10-25	J110508.11+444447.1	0.022	3.62	-19.99	21.47	0.02	8.27
NA10-29	J132852.21+110549.1	0.015	3.28	-18.12	22.29	0.34	8.38
NA10-31	J114830.64+124347.6	0.013	4.66	-17.76	22.77	0.26	8.50
NA10-33	J140156.74+122249.7	0.023	3.79	-19.36	21.92	0.20	8.35

**Note.** — (a) The Galactic extinction correction is performed. (b) Since the spectrum appears to be very noisy, we do not include this object in our zGIG sample.

- Brown, T. M., Tumlinson, J., Geha, M., et al. 2013, arXiv:1310.0824  
Chilingarian, I. V., & Zolotukhin, I. Yu. 2012, MNRAS, 419, 1727  
Cullen, F., Cirasuolo, M., McLure, R. J., & Dunlop, J. S. 2013, arXiv:1310.0816  
Dale, D. A., Cohen, L. C., Johnson, M. D., et al. 2009, ApJ, 503, 517  
Denicoló, G., Terlevich, R., & Terlevich, E. 2002, MNRAS, 330, 69  
Ferguson, H. C., Dickinson, M., Giavalisco, M., et al. 2004, ApJ, 600, L107  
Fukugita, M., Nakamura, O., Okamura, S., et al. 2007, AJ, 134, 579 (F07)  
Furusawa, H., Kosugi, G., Akiyama, M., et al. 2008, ApJS, 176, 1  
Gallagher, J. S., III, & Hunter, D. A. 1984, ARA&A, 22, 37  
Ho, L. C., Filippenko, A. V., & Sargent, W. L. W. 1997, ApJ, 487, 579  
Hubble, E. P. 1926, ApJ, 64, 321  
Hubble, E. P. 1936, The Realm of the Nebulae (New Haven, CT: Yale Univ. Press)  
Hunter, D. A., Ficut-Vicas, D., Ashley, T., et al. 2012, AJ, 144, 134  
Hunter, D. A., & Elmegreen, B. G. 2004, AJ, 128, 2170  
Hunter, D. A., & Gallagher, J. S., III 1986, PASP, 98, 5  
Impey, C. D., Sprayberry, D., Irwin, M. J., & Bothun, G. D. 1996, ApJS, 105, 209  
Kashikawa, N., Shimasaku, K., Yasuda, N., et al. 2004, PASJ, 56, 1011  
Kauffmann, G., Heckman, T. M., White, S. D. M., et al. 2003a, MNRAS, 341, 33  
Kauffmann, G., Heckman, T. M., Tremonti, C., et al. 2003b, MNRAS, 346, 1055  
Kewley, L. J., & Ellison, S. L. 2008, ApJ, 681, 1183  
Kewley, L. J., Dopita, M. A., Sutherland, R. S., Heisler, C. A., & Trevena, J. 2001, ApJ, 556, 121  
Kormendy, J., & Richstone, D. 1995, ARA&A, 33, 581  
Kormendy, J., & Ho, L. C. 2013, ARA&A, 51, 511  
Magorrian, J., Tremaine, S., Richstone, D., et al. 1998, AJ, 115, 2285  
Nair, P. B., & Abraham, R. G. 2010, ApJS, 186, 427 (NA10)  
Pettini, M., & Pagel, B. E. J. 2004, MNRAS, 348, L59  
Roberts, M. S., & Haynes, M. P. 1994, ARA&A, 32, 115  
Sandage, A. 1961, The Hubble Atlas of galaxies, Washington: Carnegie Institution, 1961  
Sanders, D. B., & Mirabel, I. F. 1996, ARA&A, 34, 749  
Schmidt, M. 1968, ApJ, 151, 393  
Scoville, N., Aussel, H., Brusa, M., et al. 2007, ApJS, 172, 1



Taniguchi, Y., Scoville, N., Murayama, T., et al. 2007, ApJS, 172, 9  
Taniguchi, Y., Murayama, T., Scoville, N. Z., et al. 2009, ApJ, 701, 915  
Theys, J. C., & Spiegel, E. A. 1976, ApJ, 208, 650  
Toomre, A., & Toomre, J. 1972, ApJ, 178, 623  
van Dokkum, P. G., Franx, M., Kriek, M., et al. 2008, ApJ, 677, L5  
Veilleux, S., & Osterbrock, D. E. 1987, ApJS, 63, 295  
White, S. D. M., & Frenk, C. S. 1991, ApJ, 379, 52  
York, D. G., Adelman, J., Anderson, J. E., Jr., et al. 2000, AJ, 120, 1579